Isoalantolactone induces autophagic cell death in $SKOV_3$ human ovarian carcinoma cells via upregulation of PEA-15

ZHIYONG WENG[1*], HONGGUO GAO[2*], JIEHUA HU[3], YONGGANG FAN[1], HONGYAN WANG[2] and LIHUA LI[1]

[1]Department of Cell Biology, Liaoning Medical University, Jinzhou, Liaoning 121001; [2]Department of Clinical Laboratory, Daqing Oilfield General Hospital, Daqing 163001; [3]Educational Technologies and Simulation Training Centre, Naval University of Engineering Tianjin Campus, Tianjin 300450, P.R. China

Received September 17, 2015; Accepted October 26, 2015

DOI: 10.3892/or.2015.4461

Abstract. We investigated the effects of isoalantolactone on cell growth inhibition and underlying cell death mechanisms in $SKOV_3$ human ovarian cancer cells. The effects of isoalantolactone on cell proliferation and cell cycle were examined by EdU incorporation assay and DNA content assay. Western blotting was performed to determine the protein expression effects of isoalantolactone on cell cycle-related proteins, autophagic regulators and PEA-15. Autophagic vacuoles were observed by acridine orange staining. PEA-15 knockdown by siRNA was used to confirm that PEA-15 was involved in isoalantolactone-induced autophagy of $SKOV_3$ cells. Isoalantolactone inhibited the viability and proliferation of $SKOV_3$ cells in a dose- and time-dependent fashion. Isoalantolactone induced cell cycle arrest at G2/M phase and decreased the expression of cell cycle-related proteins cyclin B1 and CDK1 in $SKOV_3$ cells. Accordingly, isoalantolactone also induced $SKOV_3$ cell autophagy via accumulation of autophagic vacuoles in the cytoplasm, increased Beclin1 protein expression, and increased LC3 cleavage. Furthermore, we observed that isoalantolactone-induced autophagy was through increased PEA-15 expression and the phosphorylation of ERK, whereas less change was observed to autophagy on $SKOV_3$ cells through PEA-15 knockdown by siRNA. Isoalantolactone-induced autophagic cell death was further confirmed by pretreatment with the autophagy inhibitor 3-methyladenine (3-MA). In conclusion, isoalantolactone induced cell cycle arrest and autophagy and inhibited cell proliferation of $SKOV_3$ cells via the upregulated PEA-15 expression and the phosphorylation of ERK.

Correspondence to: Professor Lihua Li, Department of Cell Biology, Liaoning Medical University, 40 Songpo Road, Jinzhou, Liaoning 121001, P.R. China
E-mail: lilihua1018@sina.com

*Contributed equally

Key words: isoalantolactone, autophagy, $SKOV_3$ cells, PEA-15 upregulation, p-ERK

Introduction

Ovarian cancer is the fifth leading cause of cancer death among women and is the primary cause of death from gynecological malignancies (1). For ovarian cancer in early phase, appropriate surgical staging and adjuvant chemotherapy for selected cases will lead to survival rates of 90-95% (2), while for advanced phase, although most patients will achieve a complete clinical response after maximal surgery together with chemotherapy at first, nearly 50% of patients will eventually develop recurrent disease (3) and the subsequent acquired chemoresistance (4-6) cause low cure rates and severely limit successful treatment (7). The difficulty in achieving an early diagnosis and the aggressive nature of this type of cancer together with the resistance limit the efficacy of surgical operation with the 5-year survival rate approximately 45% (8). Therefore, finding of novel and promising agents without resistance is urgent for the treatment of ovarian cancer.

Sesquiterpene lactone compounds are known as important botanical natural compounds have been widely used in cancer clinical trials for breast, colorectal, kidney, prostate, acute myeloid leukemia, acute lymphoblastic leukemia, non-small lung cancer (9,10), gynecologic tumors (11) and pancreatic cancer (12). Isoalantolactone is a sesquiterpene lactone isolated from the roots of *Inula helenium* L. that possesses anti-inflammatory, anti-bacterial, anti-fungal, anti-insecticidal activities with low toxicity (9,13,14). Recent reports demonstrated that isoalantolactone inhibits growth and induces apoptosis in pancreatic cancer cells in association with increased generation of reactive oxygen species (12), and our high throughput screening performance showed the anti-$SKOV_3$ cell effect of isoalantolactone. However, the anti-ovarian cancer potential of isoalantolactone compounds and their mechanism of action have not been fully elucidated.

Autophagy is a mode of cell death referred to as type II programmed cell death compared with the apoptosis pathway which is the type I programmed cell death (15), it is recognized as a cellular process of lysosome-dependent cellular catabolic degradation when cells are under various physiological and stress conditions, such as hypoxia (16), nutritional deprivation (17), radiation (18,19), chemotherapeutic agents and viral infection, and is characterized by the sequestration of bulk cytoplasm and organelles in double-membrane autophagic

vesicles and has essential roles in survival, development and homeostasis. Autophagy is also integral to human health and is involved in physiology, development, lifespan and a wide range of diseases, including cancer, neurodegeneration and microbial infection. Data from several studies concerning the expression of PEA-15 in ovarian cancer cells demonstrated that PEA-15 expression inhibited ovarian cancer proliferation via induced autophagy but not via apoptosis (20). PEA-15 is a 15 kDa small non-catalytic protein that contains a death effector domain (DED) with an irregularly structured C-terminal tail, regulating various cellular processes, such as apoptosis, cell proliferation and glucose metabolism (21).

Several natural compounds such as avicins, curcumin and evodiamine (22) can induce autophagic cell death. Recently, the induction of autophagic cell death has been studied as a potential method for cancer therapy. Therefore, we designed this study to investigate whether autophagy is involved in the antitumor effects of isoalantolactone in human ovarian cancer $SKOV_3$ cells and to further elucidate whether the antitumor activity of isoalantolactone is mediated by the up-regulation of PEA-15, which induces autophagy via activation of the ERK signaling pathway.

Materials and methods

Reagents. Isoalantolactone was purchased from Tauto Biotech Company (Shanghai, China), purity >99% as determined by analytical HPLC. Propidium iodide (PI), dimethylsulfoxide (DMSO), acridine orange dye (AO), 3-methyladenine (3-MA), trypan blue dye, cell culture media (McCoy's 5A medium, RPMI-1640 medium), pentobarbital sodium, fetal bovine serum (FBS), penicillin and streptomycin were purchased from Sigma-Aldrich (Beijing, China). Cell-Light EdU imaging detection kit was purchased from RiboBio (Guangzhou, China). On-TARGETplus SMARTpool siRNA for PEA-15 kit was purchased from Dharmacon (Lafayette, CO, USA). Lipofectamine 2000 kit, TRIzol reagent and the Primescript™ reverse transcription reagent kit were purchased from Invitrogen (Beijing, China). SYBR Premix Ex *Taq*™ II was purchased from Takara (Dalian, China). Polyclonal anti-human Beclin1, PEA-15, ERK, pERK, LC3 antibodies were purchased from Cell Signaling Technology (Beverly, MA, USA). Antibodies specific to β-actin, α-tubulin and horseradish peroxidase-conjugated secondary antibodies were purchased from Santa Cruz Biotechnology (Santa Cruz, CA, USA).

Cell culture. The human ovarian cancer cell line $SKOV_3$ was purchased from the American Type Culture Collection (ATCC, Manassas, VA, USA). The cells were maintained in McCoy's 5A medium containing 10% FBS and 1% penicillin/streptomycin at 37˚C in a humidified atmosphere containing 5% CO_2. Cell detachments were achieved by rinsing with 0.05% trypsin/0.02% EDTA solution. The cells were treated with different concentrations of isoalantolactone dissolved in DMSO with a final concentration of 1% for 24 h. DMSO-treated cells were used as a control.

Splenocytes isolation. Eight-week-old, C57/BL6 mice, weighing 20 g were used. The mice were maintained in a specific pathogen-free grade animal facility on a 12-h light/dark cycles at 22±2˚C. The mouse procedures were approved by the Experimental Animal Committee of Liaoning Medical University. Mice were anesthetized using pentobarbital sodium (65 mg/kg i.p.) and were perfused transcardially with PBS. Following midline abdominal incision spleen was removed and the freshly isolated splenocytes were cultured in RPMI-1640 medium supplemented with 20% heat-inactivated FBS and maintained at 37˚C with 5% CO_2 in a humidified atmosphere.

Cell viability and proliferation assay. For the *in vitro* cell viability experiments, a trypan blue exclusion assay was performed using Vi-CELL series cell viability analyzers (Beckman Coulter Inc., Brea, CA, USA). To determine the inhibition effect of isoalantolactone on $SKOV_3$ cell growth, cells were incubated with 35 or 75 μM isoalantolactone for 24 h. Subsequently, the cells were collected and washed with PBS and then incubated with 0.04% trypan blue for 5 min at room temperature. Trypan blue only stains dead cells. After washing, the cells were resuspended in PBS and the percentage of living and dead cells were counted. The living cell rate (%) = number of living cells/number of living cells + number of dead cells) x100.

To analyze cell proliferation for isoalantolactone treatment, cells were treated as described above. Then cell proliferation was examined by the 5-ethynyl-2-deoxyuridine (EdU) incorporation assay using the Cell-Light EdU imaging detection kit according to manufacturer's instructions.

Cell cycle analysis. $SKOV_3$ cells were incubated with 35 and 75 μM isoalantolactone for 24 h. Then the cells were collected, fixed, stained with PI staining solution (3.8 mM sodium citrate, 50 μg/ml PI in PBS) and 20 g/ml RNase A in the dark for 30 min. Cell cycle distribution was assessed by flow cytometry (Beckman Coulter, Epics XL). For the flow cytometric analysis, at least 10,000 cells were used for each sample. The data were analyzed using Cell Quest software (Becton Dickinson, San Jose, CA, USA) to measure the DNA content of cells in the G0/G1, S and G2/M phases.

Acridine orange staining. Cells ($2x10^6$) were stained with AO according to a published procedure (23). Briefly, after the cells were treated with 35 and 75 μM isoalantolactone for 24 h, the cells were incubated with 1 mg/ml AO for 20 min in the dark at 37˚C. Subsequently, the cells were washed twice with PBS. Images of the cells were obtained by fluorescence microscopy.

Acidic vesicular organelle (AVO) quantification and analysis. Cells were collected after treatment with 35 and 75 μM isoalantolactone in the presence or absence of the autophagy inhibitor 3-methyladenine (3-MA 5 mM) for 24 h. Next, the cells were incubated with 1 mg/ml AO for 20 min in the dark at 37˚C. After washing, the cells were analyzed by flow cytometry and CellQuest software. Red fluorescence emissions from 10^6 cells were analyzed, and quantified as percentage of cells containing AVOs.

siRNA silencing of PEA-15. In all, $5x10^5$ cells were seeded in 6-well plates. After 24 h, the cells were transfected with siRNA using Lipofectamine 2000. After 3 days, the trans-

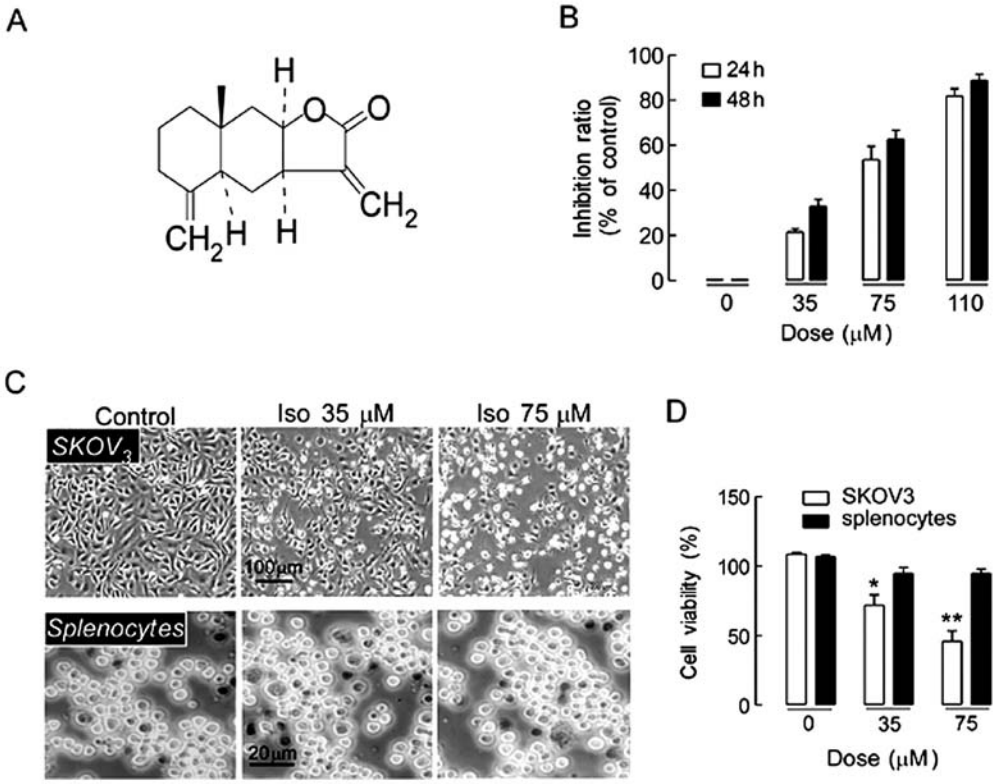

Figure 1. Chemical structure and inhibitory effects of isoalantolactone on the growth of $SKOV_3$ cells and mouse splenocytes. (A) Chemical structure of isoalantolactone. (B) $SKOV_3$ cells were treated with various concentrations of isoalantolactone for 24 and 48 h. Then cell growth inhibition assays were performed using trypan blue exclusion method. The data shown are the means ± SEM (n=3). (C, top) Morphological changes in $SKOV_3$ cells observed via phase-contrast microscopy after treating cells with various concentrations of isoalantolactone for 24 h. (C, down) Mouse splenocytes were treated with isoalantolactone for 24 h, and dead and live cells were observed microscopically by trypan blue staining. (D) The viability of $SKOV_3$ cells and splenocytes treated with different isoalantolactone doses is showed as means ± SEM (n=3), $^{*}P<0.05$, $^{**}P<0.01$ compared with the control.

fected cells that were treated with isoalantolactone or DSMO were collected for the clonogenic survival assay and western blot analysis.

Immunoblot analysis. Cells were treated with isoalantolactone for 24 h, washed twice with PBS, and lysed on ice with WIP cell lysis reagent supplemented with 1% PMSF for 30 min. The insoluble protein lysate was removed by centrifugation at 12,000 rpm for 15 min at 4˚C. The protein concentrations were determined using a NanoDrop 1000 spectrophotometer (Thermo Scientific, Waltham, MA, USA). Proteins (20 μg) were electrophoresed using 10% SDS-PAGE gels and transferred to a PVDF membrane. After blocking with 5% non-fat milk and washing with a Tris-buffered saline/Tween solution (TBST), the membranes were incubated overnight at 4˚C with specific primary antibodies and then with anti-rabbit IgG or anti-mouse IgG secondary antibodies for 1 h at room temperature. Signals were detected using the ECL plus chemiluminescence kit and X-ray film (Millipore Billerica, MA, USA). All the bands obtained were quantified by densitometry using ImageJ software.

Statistical analysis. The results are expressed as the means ± SEM. Analyses were performed using GraphPad prism 5 software. One-way analysis of variance (ANOVA) was used to analyze significant differences between groups under different conditions. Student's t-test was used to determine significance when only two groups were compared and $P<0.05$ was considered to indicate a statistically significant difference.

Results

Effects of isoalantolactone on the growth inhibition on the $SKOV_3$ cells and normal mouse splenocytes. The chemical structure of isoalantolactone is shown in Fig. 1A. $SKOV_3$ cells were treated with different doses of isoalantolactone (0, 35, 75, or 110 μM) for 24 and 48 h. As shown in Fig. 1B, isoalantolactone significantly inhibited the growth of $SKOV_3$ cells in a dose- and time-dependent manner. To further confirm the effect of isoalantolactone on growth inhibition, cellular morphology changes were observed using inverted phase contrast microscopy. The cells became rounder and shrunken, and they floated in the culture medium as the concentration of isoalantolactone increased (Fig. 1C), supporting the finding that isoalantolactone inhibited $SKOV_3$ cell growth in a dose-dependent manner. The cytotoxic effect of isoalantolactone was further evaluated by trypan blue staining on normal mouse splenocytes. The data showed that fewer inhibitory effects were observed in splenotypes treated with isoalantolactone at different doses (Fig. 1C), suggesting that $SKOV_3$ cells are more sensitive than normal cells to isoalantolactone. The effect of isoalantolactone at different concentrations on the viability of $SKOV_3$ cells was assessed by live/death cells staining. As Fig. 1D shows, isoalantolactone inhibited $SKOV_3$ cells growth in a dose-dependent

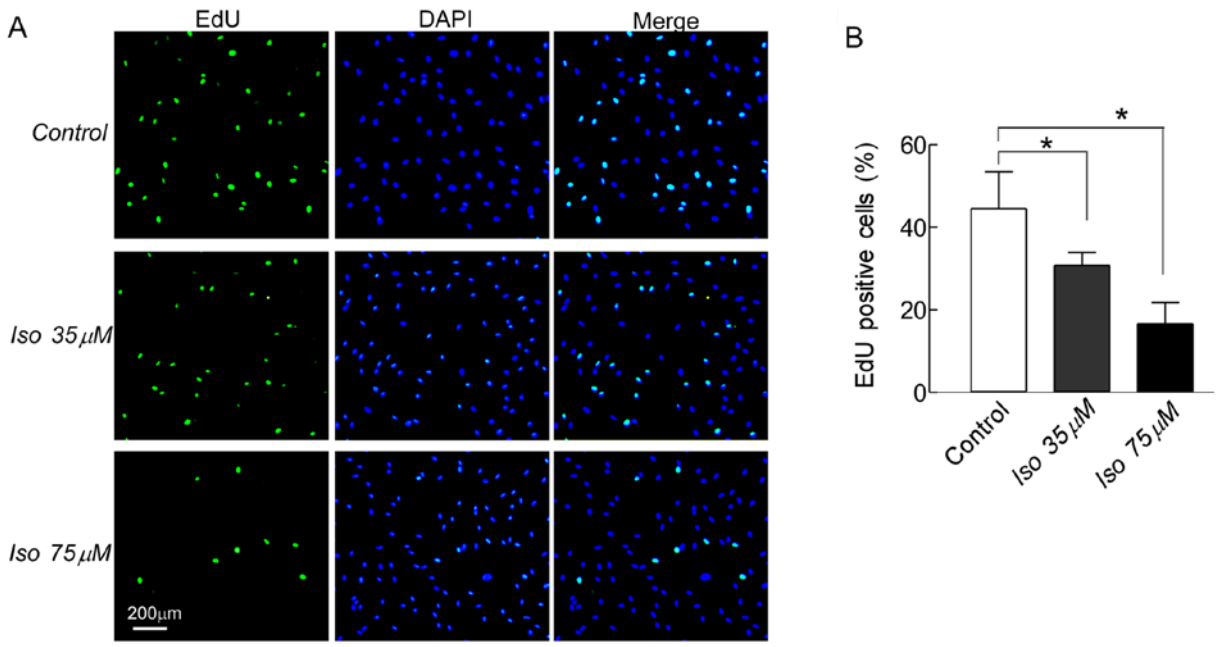

Figure 2. Isoalantolactone inhibits the proliferation of SKOV$_3$ cells. (A) SKOV$_3$ cells were treated with different concentrations of isoalantolactone for 24 h. The proliferative ability of SKOV$_3$ cells was examined using EdU incorporation assays. (B) The isoalantolactone-inhibited proliferation of SKOV$_3$ cells is shown as means ± SEM (n=3), *P<0.05 compared with the control.

manner. The data indicated that isoalantolactone was able to inhibit SKOV$_3$ cell growth selectively.

Effects of isoalantolactone on the cell proliferation of SKOV$_3$ cells. To further confirm that isoalantolactone inhibited SKOV$_3$ cell growth, we tested the cell proliferation using the EdU incorporation assay. Fig. 2A shows the EdU-positive cells on SKOV$_3$ cells treated with 35 or 75 μM isoalantolactone for 24 h. Compared to the control group (48.2%), the EdU-positive cells in the isoalantolactone-treated groups at 35 (27.4%, P<0.05) or 75 μM (16.6%, P<0.05) were significantly reduced in a dose-dependent manner (Fig. 2B). Thus, isoalantolactone shows promise as an antitumor drug for human ovarian cancer.

Effects of isoalantolactone on the cell cycle and cell cycle-related proteins in SKOV$_3$ cells. One of the major mechanisms underlying the anti-proliferative effect of anticancer drugs is the prevention of cell cycle progression. To explore the possible mechanism underlying the inhibitory effect of isoalantolactone on the growth of SKOV$_3$ cells, cell cycle distribution was examined by flow cytometry to analyze the DNA content of cell cycle phase. As shown in Fig. 3A, isoalantolactone induced a dose-dependent increase in the number of SKOV$_3$ cells in G2/M phase, the percentage of accumulation of cells was increased from 20.8% in the control group to 33.2% (P<0.05) and 46.3% (P<0.01) in the cells treated with 35 and 75 μM of isoalantolactone, respectively for 24 h, leading to a decrease in the proportion of cells in G0/G1 phase from 41.9% in the control group to 27.9% (P<0.05) and 20.6% (P<0.01) in the cells with the above-mentioned different concentration (Fig. 3B). We also investigated the expression of cyclin B1 and CDK1 of cell cycle regulators by western blot analysis. The results revealed that the expression of cyclin B1 and CDK1 were gradually decreased with increasing concentrations of isoalantolactone in a dose-dependent manner (Fig. 3C), indicating that cell cycle arrest at G2/M phase may be associated with the inhibition of SKOV$_3$ cell growth by isoalantolactone treatment.

Effects of isoalantolactone on AVO formation in SKOV$_3$ cells. Autophagy is closely associated with tumors and plays an important role in human tumor suppression. AVO formation (autophagosomes and autolysosomes) is a characteristic feature of autophagy (24). To investigate whether autophagy was involved in the inhibitory effects of isoalantolactone on SKOV$_3$ cell growth, the accumulation of AVOs was analyzed by AO staining and quantified by flow cytometry (25). AO has a weak base that freely passes across the plasma membrane in a neutral state distinguished by green fluorescence. After entrance into acidic compartments, AO changes into the protonated form which is distinguished by bright red fluorescence while control cells primarily showed green fluorescence. The intensity of the red fluorescence was proportional to the degree of acidity. Thus, the formation of AVOs could be quantified. As shown in Fig. 4A, after cell treatment with isoalantolactone, the intensity of the bright red fluorescence was markedly increased in a dose-dependent manner compared to the control. We further quantified AVOs by flow cytometry. Fig. 4B illustrates significant formation of AVOs in isoalantolactone-treated cells (26.5 or 39.2%, P<0.01) compared to the control cells (2.1%). Accordingly, we added the autophagy inhibitor 3-MA, which controls the autophagy pathway at various points (26). We found that isoalantolactone-induced AVO formation was suppressed when the cells were treated in combination with the specific autophagy inhibitor (28.8%, P<0.05) (Fig. 4C). These results show that isoalantolactone-induced autophagy is involved in inducing death of SKOV$_3$ cells.

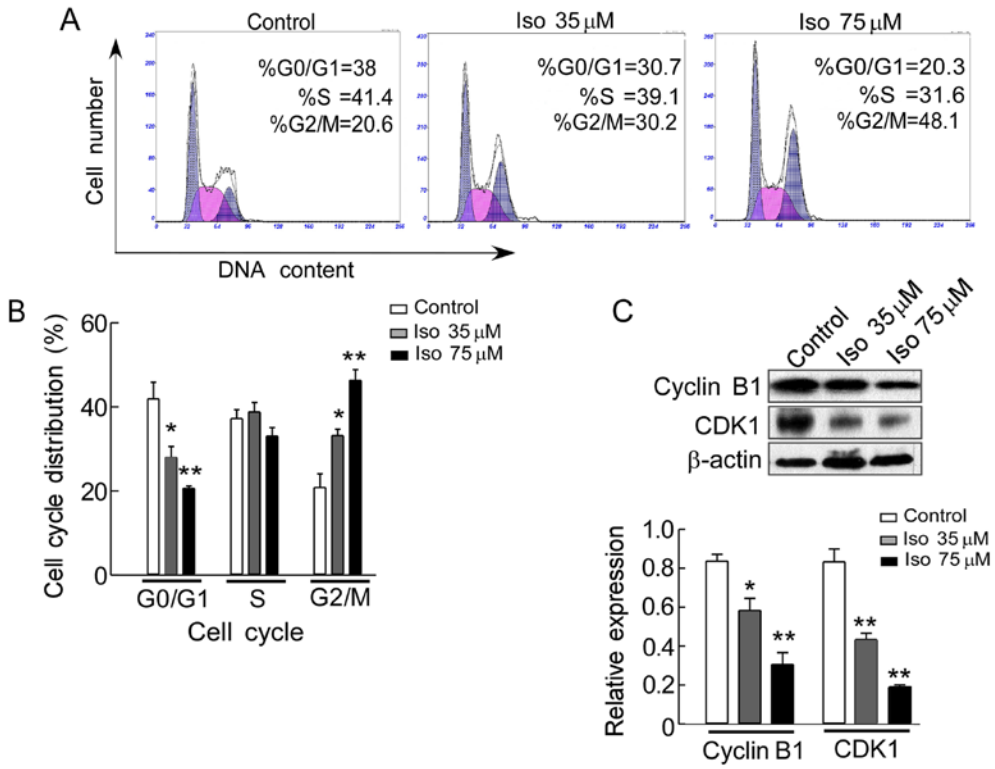

Figure 3. Effects of isoalantolactone on cell cycle distribution and cell cycle-related proteins in $SKOV_3$ cells. (A) $SKOV_3$ cells were treated with 35 and 75 μM isoalantolactone for 24 h. The DNA content in each cell cycle phase was analyzed by flow cytometry. Histograms show the number of cells/channel (y-axis) vs. DNA content (x-axis). (B) Isoalantolactone induced G2/M phase of cell cycle arrest in $SKOV_3$ cells. The results are presented as the means ± SEM of at least 3 measurements from independent experiments with similar results (n=3). *P<0.05, **P<0.01 compared with the control. (C) Expression of Cyclin B1 and CDK1 was examined by western blot analysis. β-actin was used as a control. The values were expressed as means ± SEM of at least 3 measurements from independent experiments. *P<0.05, **P<0.01 compared with control.

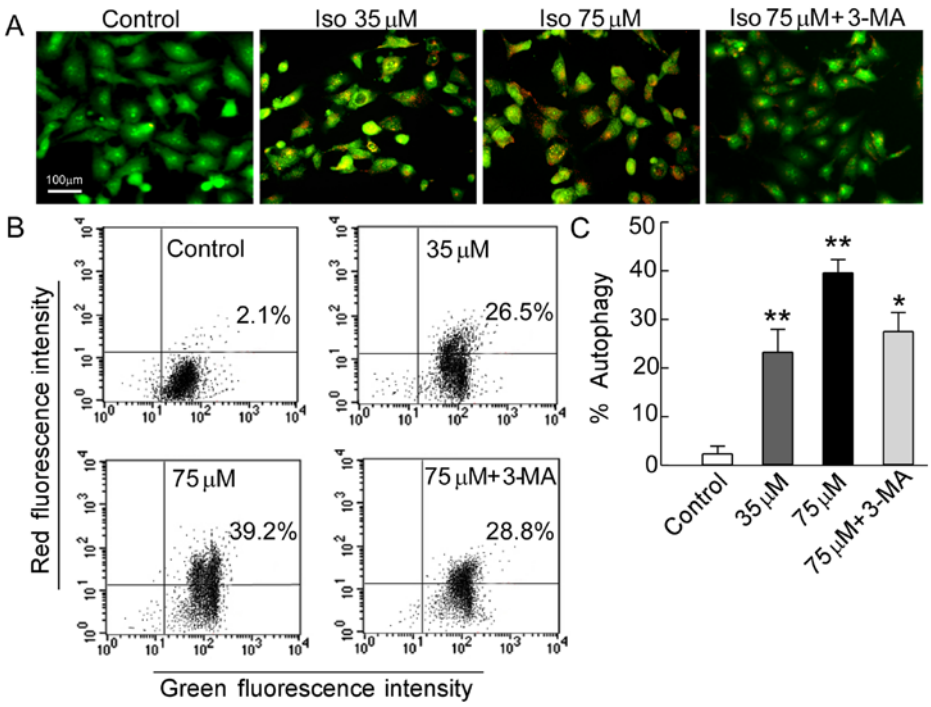

Figure 4. Induction of autophagy on $SKOV_3$ cells by isoalantolactone. (A) AVOs stained with AO in isoalantolactone-treated $SKOV_3$ cells. Autophagy inhibitor 3-MA was used in combination with 75 μM isoalantolactone. Green color intensity shows the cytoplasm and the nucleus, while red color intensity shows AVOs. (B) Development of AVOs in isoalantolactone-treated $SKOV_3$ cells. Green and red fluorescence in AO staining cells were detected using flow cytometry. Representative histograms are from $SKOV_3$ cells incubated with different concentrations of isoalantolactone or autophagy inhibitor 3-MA. (C) Quantification of autophagic cells in isoalantolactone-treated $SKOV_3$ cells. The percentage of autophagy was quantified by counting the number of cells showing red fluorescence. Results shown are the means ± SEM of at least 3 measurements from independent experiments with similar results. *P<0.05 compared with 75 μM isoalantolactone; **P<0.01 compared to the control.

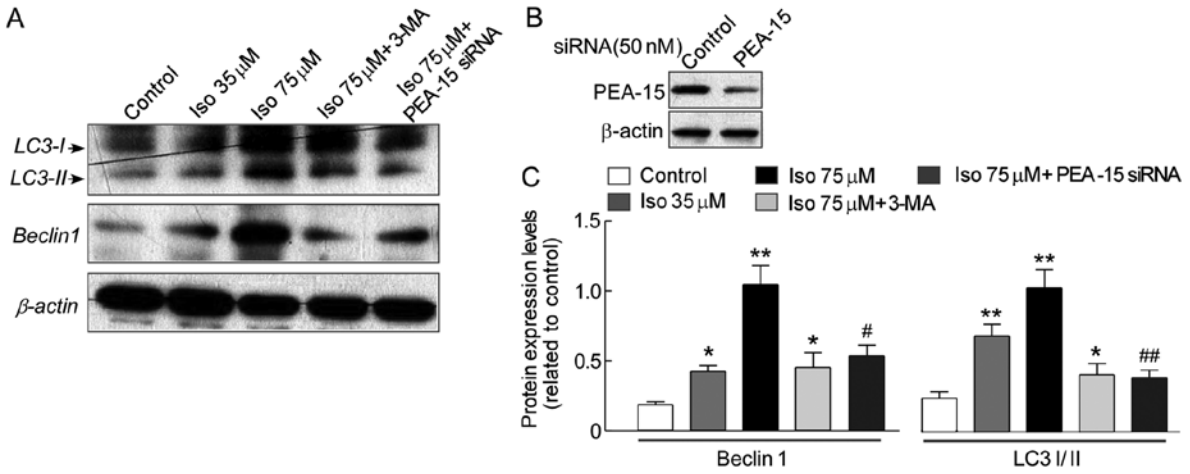

Figure 5. Effects of isoalantolactone on the expression of autophagy proteins. (A) Isoalantolactone upregulates the expression of LC3-I, LC3-II and Beclin1 proteins in SKOV$_3$ cells as evidenced by western blot analysis. 3-MA markedly reduced the expression of LC3-I, LC3-II and Beclin1 in SKOV$_3$ cells treated with high-dose isoalantolactone. β-actin was used as a control for protein level. (B) Cells were transfected with Lipofectamine 2000 siRNA targeting PEA-15. Seventy-two hours later, one portion of cells was for immunoblotting. PEA-15 was knockdown to ~50% of the original level. (C) The data are presented as the means ± SEM of at least 3 measurements from independent experiments. *P<0.05, **P<0.01, compared with the control; $^{\#}$P<0.05, $^{\#\#}$P<0.01 compared with 75 μM isoalantolactone.

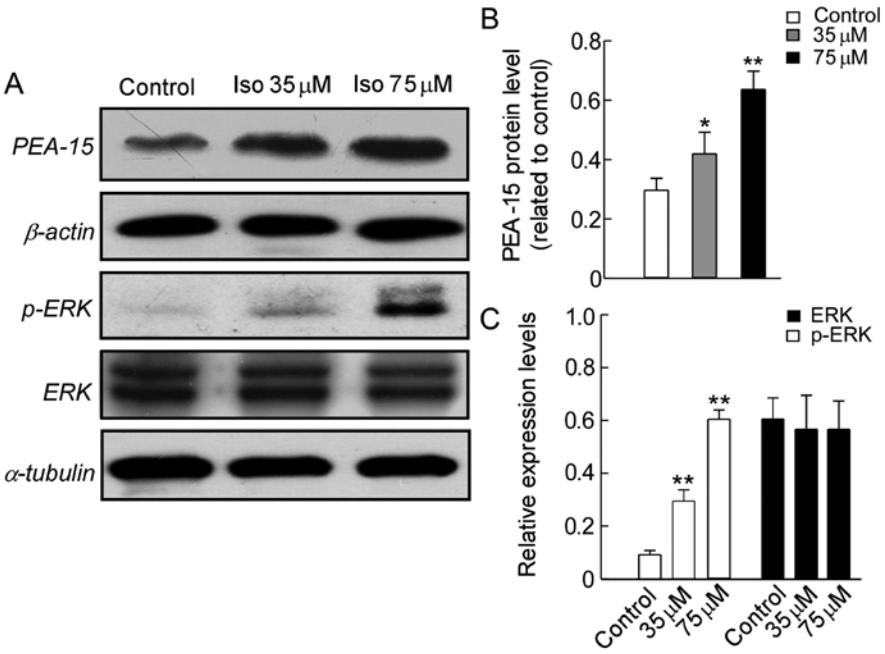

Figure 6. Effects of isoalantolactone on the expression of autophagy regulators. (A) Representative images of western blots showing PEA-15, ERK and pERK protein expression. β-actin and α-tubulin were used as a control for protein level. (B) The data are presented as the means ± SEM of at least 3 measurements from independent experiments with similar results (n=3). *P<0.05, **P<0.01 compared with the control.

Effects of isoalantolactone on the expression of autophagy proteins in SKOV$_3$ cells. To further confirm involvement of autophagy in isoalantolactone-induced SKOV$_3$ cell death, Western blot analysis was performed to evaluate the effects of isoalantolactone on the autophagy protein expression of Beclin1, which was the initiation factor of autophagosome formation, LC3-I and LC3-II (autophagosome marker). As shown in Fig. 5, isoalantolactone activated Beclin1 expression and increased the ratio of LC3-I and LC3-II protein expression in a dose-dependent manner, while markedly decreased in cells pre-treated with the combination 3-MA and 75 μM isoalantolactone compared to cells treated only with 75 μM isoalantolactone, confirming that autophagy was involved in isoalantolactone-induced cell death.

Effects of isoalantolactone on the expression of autophagy regulators in SKOV$_3$ cells. Autophagy is a complicated regulatory process, which involves a great number of upstream regulating signaling pathways (27,28). While ERK, the target of PEA-15, is relatively new regulator studied of autophagy (20,29,30). To elucidate the underlying mechanism of autophagy induced by isoalantolactone in SKOV$_3$ cells, we examined the expression of PEA-15, ERK and pERK by western blot analysis. As shown in Fig. 6A and B, isoalanto-

lactone greatly increased PEA-15 expression and activated ERK phosphorylation in a dose-dependent manner compared to the control cells, whereas no great change on ERK total protein level was seen (Fig. 6C). These results suggest that isoalantolactone-induced upregulation of PEA-15 expression and activation of ERK signaling pathway are associated with autophagy in $SKOV_3$ cells.

PEA-15 knockdown by siRNA depresses autophagy of $SKOV_3$ cells by isoalantolactone induction. Based on the results described above, we further confirm whether isoalantolactone induced autophagy on $SKOV_3$ cells through upregulation PEA-15 expression. The PEA-15 knockdown was performed by siRNA. Indeed, PEA-15 knockdown to ~50% of the original level significantly reduced AVO formation of $SKOV_3$ cells by isoalantolactone induction (Fig. 5B). Western blot analysis showed that the expression of Beclin1, LC3-I and LC3-II protein levels on $SKOV_3$ cells were greatly decreased by PEA-15 knockdown compared to cells treated with high-dose isoalantolactone ($P<0.05$ or $P<0.01$) (Fig. 5C). Thus, the PEA-15 levels correlated with isoalantolactone-induced autophagy on $SKOV_3$ cells.

Discussion

In the present study, high throughput screening of a library of compounds derived from Chinese herbs was performed using $SKOV_3$ human ovarian cancer cells. Isoalantolactone, a sesquiterpene lactone compound, was identified as a potent growth inhibitor of $SKOV_3$ cells during the screening process. After the cells were treated with isoalantolactone for 24 h, the IC_{50} value was 55 μM. Cell proliferation analysis revealed that isoalantolactone inhibited $SKOV_3$ cell growth in a dose- and time-dependent manner, whereas, did not display a significant toxic effect on normal mouse splenocytes *in vitro*, which indicates the growth-inhibiting effect of isoalantolactone was selective to tumor cells.

Cell cycle arrest, apoptosis and autophagy are main causes of cell proliferation inhibition (30). Obstruction of cell cycle progression in cancer cells is considered as one of the most effective strategies for the control of tumor growth (31). We first investigated whether the inhibitory effect of isoalantolactone on $SKOV_3$ cell growth was due to cell cycle arrest. Flow cytometry showed that isoalantolactone blocked $SKOV_3$ cells in the G2/M phase of the cell cycle in a dose-dependent manner, suggesting that retardation of cell cycle progression may be one of the mechanisms underlying the antiproliferative effect of isoalantolactone. In addition, we also analyzed cellular apoptosis by isoalantolactone induction in $SKOV_3$ cells. Flow cytometric analysis showed that less apoptotic cells are observed by isoalantolactone induction (data no shown). These data indicate that isoalantolactone induced $SKOV_3$ cell death through cell cycle arrest in G2/M phase, but independently of the induction of apoptosis.

Autophagy is a major pathway for bulk degradation of proteins within the lysosome/vacuole compartments. This pathway initiates the formation of the pre-autophagosome that enwraps part of the cytoplasm to form a double membrane autophagosome, which is then transported to the lysosome/vacuole for degradation (32,33). The AVO formation is one of the characteristic features of cells which pass through the process of autophagy after exposure to different autophagy inducer agents (34). Beclin1 was part of the class III PI3K complex that promotes autophagy, functions as a tumor suppressor in mammalian cells and was essential for the double-membrane autophagosome formation, which was required during the initial steps of autophagy (35). The autophagic induction of Beclin1 facilitates the inhibition of tumorigenesis (28). The allelic loss of Beclin1 is frequently seen in human breast, ovarian and prostate cancers (36). LC3 (microtubule-associated protein 1 light chain 3) was one of the most important mammalian homologue of yeast Atg8 (37) which was cleave by the protease ATG4 and then conjugated to the lipid phosphatidyl ethanolamine via the activity of ATG7 and ATG3. While the unprocessed form of LC3 (LC3I) was diffusely distributed throughout the cytoplasm, the lipidated form of LC3 (LC3II) specifically accumulates on nascent autophagosomes to promote membrane fusion and thus represents a marker to monitor autophagy (38).

Thus, we observed the effect of isoalantolactone induction on the formations of AVOs in $SKOV_3$ cells using lysosomotropic agent AO staining and the expression of autophagy related proteins using western blot analysis. Our results showed accumulation of AVOs in the cytoplasm, and increased expression of the Beclin1 protein as well as that ratio of the LC3-I, LC3-II proteins occurred in a dose-dependent manner, whereas, respective, the decrease was accompanied by treatment with an autophagy inhibitor 3-MA following treatment with isoalantolactone, demonstrating that autophagy was involved in isoalantolactone-induced cell death in $SKOV_3$ cells.

Accordingly, previous studies showed that ovarian cancer cell proliferation was inhibited by the expression of PEA-15, which blocks ERK-dependent proliferation by sequestering ERK in the cytoplasm and preventing its entry into the nucleus (39). Previous reports indicated that the antitumor activity of PEA-15 in ovarian cancer cells was due to induction of autophagy via activated pERK (20). Moreover, ERK was shown to phosphorylate Gα-interacting protein to induce autophagy in human colon cells, and the MAPK pathway is an important regulator of autophagy (29,30). Thus further studies are needed to investigate whether the anti-proliferative activity of isoalantolactone occurs through upregulation of PEA-15 expression to induce autophagy via activated ERK phosphorylation. Our results showed that isoalantolactone-induced the upregulation of PEA-15 expression, the accumulation of AVOs in the cytoplasm, and the increased expression of the Beclin1 protein as well as that ratio of the LC3-I, LC3-II occurred in a dose-dependent manner, whereas the respective decrease was accompanied by treatment with an autophagy inhibitor or PEA-15 knockdown by siRNA. Taken together, these results support the hypothesis that isoalantolactone triggered autophagy and demonstrate that autophagy is involved in the anti-tumor effects of isoalantolactone in $SKOV_3$ cells.

In conclusion, our studies provide experimental evidence that isoalantolactone significantly inhibits the proliferation of $SKOV_3$ cells and induces G2/M phase cell cycle arrest. Furthermore, isoalantolactone-induced autophagy of $SKOV_3$ cells was through upregulation of the expression of PEA-15

and activation of the phosphorylation of ERK. These findings indicate that isoalantolactone is a potential antitumor agent for treating ovarian cancer.

Acknowledgements

The present study was supported by the National Natural Science Foundation of China (no. 31571184).

References

1. Jemal A, Siegel R, Ward E, Hao Y, Xu J and Thun MJ: Cancer statistics, 2009. CA Cancer J Clin 59: 225-249, 2009.
2. Bhoola S and Hoskins WJ: Diagnosis and management of epithelial ovarian cancer. Obstet Gynecol 107: 1399-1410, 2006.
3. Siegel R, Ward E, Brawley O and Jemal A: Cancer statistics, 2011: The impact of eliminating socioeconomic and racial disparities on premature cancer deaths. CA Cancer J Clin 61: 212-236, 2011.
4. Yagüe E, Arance A, Kubitza L, O'Hare M, Jat P, Ogilvie CM, Hart IR, Higgins CF and Raguz S: Ability to acquire drug resistance arises early during the tumorigenesis process. Cancer Res 67: 1130-1137, 2007.
5. Tsuruo T, Naito M, Tomida A, Fujita N, Mashima T, Sakamoto H and Haga N: Molecular targeting therapy of cancer: Drug resistance, apoptosis and survival signal. Cancer Sci 94: 15-21, 2003.
6. Szakács G, Paterson JK, Ludwig JA, Booth-Genthe C and Gottesman MM: Targeting multidrug resistance in cancer. Nat Rev Drug Discov 5: 219-234, 2006.
7. Ozols RF, Bookman MA, du Bois A, Pfisterer J, Reuss A and Young RC: Intraperitoneal cisplatin therapy in ovarian cancer: Comparison with standard intravenous carboplatin and paclitaxel. Gynecol Oncol 103: 1-6, 2006.
8. Ramirez I, Chon HS and Apte SM: The role of surgery in the management of epithelial ovarian cancer. Cancer Control 18: 22-30, 2011.
9. Ghantous A, Gali-Muhtasib H, Vuorela H, Saliba NA and Darwiche N: What made sesquiterpene lactones reach cancer clinical trials? Drug Discov Today 15: 668-678, 2010.
10. Zhang S, Won YK, Ong CN and Shen HM: Anti-cancer potential of sesquiterpene lactones: Bioactivity and molecular mechanisms. Curr Med Chem Anticancer Agents 5: 239-249, 2005.
11. Li Y, Ni ZY, Zhu MC, Dong M, Wang SM, Shi QW, Zhang ML, Wang YF, Huo CH, Kiyota H, *et al*: Antitumour activities of sesquiterpene lactones from *Inula helenium* and *Inula japonica*. Z Naturforsch C 67: 375-380, 2012.
12. Khan M, Ding C, Rasul A, Yi F, Li T, Gao H, Gao R, Zhong L, Zhang K, Fang X, *et al*: Isoalantolactone induces reactive oxygen species mediated apoptosis in pancreatic carcinoma PANC-1 cells. Int J Biol Sci 8: 533-547, 2012.
13. Pal HC, Sehar I, Bhushan S, Gupta BD and Saxena AK: Activation of caspases and poly (ADP-ribose) polymerase cleavage to induce apoptosis in leukemia HL-60 cells by Inula racemosa. Toxicol In Vitro 24: 1599-1609, 2010.
14. Trendafilova A, Chanev C and Todorova M: Ultrasound-assisted extraction of alantolactone and isoalantolactone from *Inula helenium* roots. Pharmacogn Mag 6: 234-237, 2010.
15. Leist M and Jäättelä M: Four deaths and a funeral: From caspases to alternative mechanisms. Nat Rev Mol Cell Biol 2: 589-598, 2001.
16. Semenza GL: Mitochondrial autophagy: Life and breath of the cell. Autophagy 4: 534-536, 2008.
17. Shintani T and Klionsky DJ: Autophagy in health and disease: A double-edged sword. Science 306: 990-995, 2004.
18. Ito H, Daido S, Kanzawa T, Kondo S and Kondo Y: Radiation-induced autophagy is associated with LC3 and its inhibition sensitizes malignant glioma cells. Int J Oncol 26: 1401-1410, 2005.
19. Paglin S, Hollister T, Delohery T, Hackett N, McMahill M, Sphicas E, Domingo D and Yahalom J: A novel response of cancer cells to radiation involves autophagy and formation of acidic vesicles. Cancer Res 61: 439-444, 2001.
20. Bartholomeusz C, Rosen D, Wei C, Kazansky A, Yamasaki F, Takahashi T, Itamochi H, Kondo S, Liu J and Ueno NT: PEA-15 induces autophagy in human ovarian cancer cells and is associated with prolonged overall survival. Cancer Res 68: 9302-9310, 2008.
21. Fiory F, Formisano P, Perruolo G and Beguinot F: Frontiers: PED/PEA-15, a multifunctional protein controlling cell survival and glucose metabolism. Am J Physiol Endocrinol Metab 297: E592-E601, 2009.
22. Rasul A, Yu B, Zhong L, Khan M, Yang H and Ma T: Cytotoxic effect of evodiamine in SGC-7901 human gastric adenocarcinoma cells via simultaneous induction of apoptosis and autophagy. Oncol Rep 27: 1481-1487, 2012.
23. Kanzawa T, Kondo Y, Ito H, Kondo S and Germano I: Induction of autophagic cell death in malignant glioma cells by arsenic trioxide. Cancer Res 63: 2103-2108, 2003.
24. Levine B and Yuan J: Autophagy in cell death: An innocent convict? J Clin Invest 115: 2679-2688, 2005.
25. Kanzawa T, Zhang L, Xiao L, Germano IM, Kondo Y and Kondo S: Arsenic trioxide induces autophagic cell death in malignant glioma cells by upregulation of mitochondrial cell death protein BNIP3. Oncogene 24: 980-991, 2005.
26. Liang XH, Jackson S, Seaman M, Brown K, Kempkes B, Hibshoosh H and Levine B: Induction of autophagy and inhibition of tumorigenesis by Beclin 1. Nature 402: 672-676, 1999.
27. Mathew R, Karantza-Wadsworth V and White E: Role of autophagy in cancer. Nat Rev Cancer 7: 961-967, 2007.
28. Chen N and Karantza-Wadsworth V: Role and regulation of autophagy in cancer. Biochim Biophys Acta 1793: 1516-1523, 2009.
29. Corcelle E, Nebout M, Bekri S, Gauthier N, Hofman P, Poujeol P, Fénichel P and Mograbi B: Disruption of autophagy at the maturation step by the carcinogen lindane is associated with the sustained mitogen-activated protein kinase/extracellular signal-regulated kinase activity. Cancer Res 66: 6861-6870, 2006.
30. Ogier-Denis E, Pattingre S, El Benna J and Codogno P: Erk1/2-dependent phosphorylation of Galpha-interacting protein stimulates its GTPase accelerating activity and autophagy in human colon cancer cells. J Biol Chem 275: 39090-39095, 2000.
31. Janssen A and Medema RH: Mitosis as an anti-cancer target. Oncogene 30: 2799-2809, 2011.
32. Mizushima N, Yamamoto A, Hatano M, Kobayashi Y, Kabeya Y, Suzuki K, Tokuhisa T, Ohsumi Y and Yoshimori T: Dissection of autophagosome formation using Apg5-deficient mouse embryonic stem cells. J Cell Biol 152: 657-668, 2001.
33. Weidberg H, Shpilka T, Shvets E, Abada A, Shimron F and Elazar Z: LC3 and GATE-16 N termini mediate membrane fusion processes required for autophagosome biogenesis. Dev Cell 20: 444-454, 2011.
34. Daido S, Kanzawa T, Yamamoto A, Takeuchi H, Kondo Y and Kondo S: Pivotal role of the cell death factor BNIP3 in ceramide-induced autophagic cell death in malignant glioma cells. Cancer Res 64: 4286-4293, 2004.
35. Cao Y and Klionsky DJ: Physiological functions of Atg6/Beclin 1: A unique autophagy-related protein. Cell Res 17: 839-849, 2007.
36. Aita VM, Liang XH, Murty VV, Pincus DL, Yu W, Cayanis E, Kalachikov S, Gilliam TC and Levine B: Cloning and genomic organization of beclin 1, a candidate tumor suppressor gene on chromosome 17q21. Genomics 59: 59-65, 1999.
37. Tanida I, Sou YS, Ezaki J, Minematsu-Ikeguchi N, Ueno T and Kominami E: HsAtg4B/HsApg4B/autophagin-1 cleaves the carboxyl termini of three human Atg8 homologues and delipidates microtubule-associated protein light chain 3- and GABAA receptor-associated protein-phospholipid conjugates. J Biol Chem 279: 36268-36276, 2004.
38. Kabeya Y, Mizushima N, Ueno T, Yamamoto A, Kirisako T, Noda T, Kominami E, Ohsumi Y and Yoshimori T: LC3, a mammalian homologue of yeast Apg8p, is localized in autophagosome membranes after processing. EMBO J 19: 5720-5728, 2000.
39. Renault F, Formstecher E, Callebaut I, Junier MP and Chneiweiss H: The multifunctional protein PEA-15 is involved in the control of apoptosis and cell cycle in astrocytes. Biochem Pharmacol 66: 1581-1588, 2003.